International Journal of Emerging Engineering Research and Technology
Volume 8, Issue 6, 2020, PP 1-12
ISSN 2349-4395 (Print) & ISSN 2349-4409 (Online)

Investigation of Colon Using Speckle and Cascaded Interferometric Techniques

A.M. Hamed*

Physics Department, Faculty of Science, Ain Shams University, Cairo, Egypt

***Corresponding Author:** A.M. Hamed, Physics Department, Faculty of Science, Ain Shams University, Cairo, Egypt*

ABSTRACT

In this paper, two different techniques are used in the investigation of colon cancer images. The 1st technique is based on modulated speckle photography computed from the Fourier diffraction of the colon image combined with the diffuser, while the 2nd technique is based on cascaded multiple beam interference. Discrimination between the colon cancer and colon polyp is obtained from the speckle images. In addition, discrimination between benign, and malignant colon cells is attained by comparing the corresponding modulated speckle profiles. The surface topography of the colon cancer can be obtained from either the fringe shift corresponding to the interference pattern or the profile shape plotted from the source input image. Finally, the refractive index corresponding to the colon malignant and benign cells is computed from the surface height variation as outlined in the analysis. All images and results are obtained making use of Mat- Lab code.

Keywords: *Cascaded multiple beam interference- modulated speckle photography- surface topography of images – Colon cancer.*

INTRODUCTION

Colon cancer: A malignancy that arises from the inner lining of the colon. Most, if not all, of these cancers develop from colonic polyps. Removal of these precancerous polyps can prevent colon cancer. Colon polyps and early colon cancers cause no signs or symptoms. Full-blown colon cancer can cause occult (a microscopic amount of) blood in the stool, overt rectal bleeding, bowel obstruction, and weight loss. Risk factors for colon cancer include a family history of it or of colonic polyps, and long standing ulcerative colitis. The overall risk can be reduced by following a diet low in fat and high in fiber. Colon cancer is preventable and curable. It is preventable by removing the precancerous colon polyps. It is curable if detected early when it can be surgically removed before it has spread to other parts of the body. If screening and surveillance programs were practiced universally, there would be a tremendous reduction in the incidence and mortality of colon cancer [1].

The image of the colon with cancerous zone in the descending colon and polyp zone in the ascending colon are shown as in the figure (1).

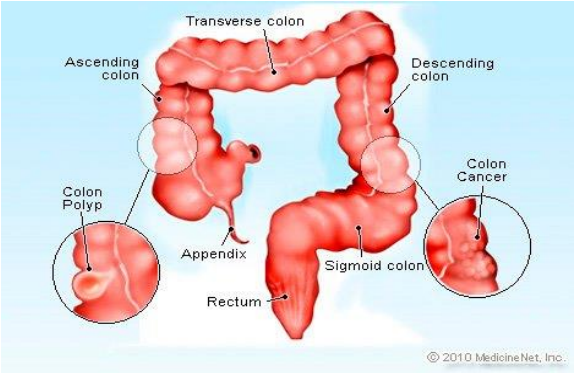

Figure1. *The colon with cancerous cells and polyps are shown in the image.*

In the most basic terms, cancer refers to cells that grow out-of-control and invade other tissues. Cells may become cancerous due to the accumulation of defects, or mutations, in their DNA. Certain inherited genetic defects and infections can increase the risk of cancer. Environmental factors (for example, air pollution) and poor lifestyle choices—such as smoking and heavy alcohol use—can also damage DNA and lead to cancer. Most of the time, cells are able to detect and repair DNA damage. If a cell is severely damaged and cannot repair itself, it usually undergoes so-called programmed cell death or apoptosis. Cancer occurs when damaged cells grow,

divide, and spread abnormally instead of self-destructing as they should.

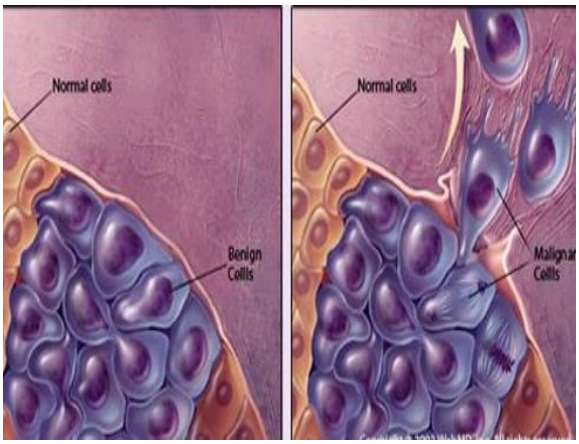

Figure2. *Malignant and benign cells are shown in the colon where in the left benign cells are shown while in the right malignant cells are shown.*

In the literature, differentiation between benign and malignant colon cancer is outlined in different articles using segmentation and image processing [2]. The benign tumors grow locally and do not spread. As a result, benign tumors are not considered cancer. They can still be dangerous, especially if they press against vital organs like the brain. While the Malignant tumors have the ability to spread and invade other tissues. This process, known as metastasis, is a key feature of cancer. There are many different types of malignancy based on where a cancer tumor originates. An image of normal, benign, and malignant colon cells is shown as in the figure (2).Recently, the image processing of colon cancer and tumors is outlined in different publications [3- 8]. Symptoms and treatment of various cancers various parts of the large intestine may differ materially. The main parts of the large intestine are: cecum, ascending colon, transverse colon, descending colon and rectum. Cancer can occur in any of these parts (mostly occurs in the rectum) [8]. Bleeding from the rectum, observed as the presence of visible blood in the stool, it should be a warning about the disorder that can be serious [3, 4]. Analysis algorithm and image processing for quantitative description of colon cancer cells is given [9]. Later on, image processing of Corona and SIDA virus using two and multiple beam interference is given in [11, 12, 13] which is improved using cascaded arrangements for interference as in [14- 17]. In addition, image processing based on speckle photography technique is given in [10, 11, 19]. In this paper, investigation of cancerous cells in colon is realized using two different techniques namely cascaded interferometry and speckle photography.

Theoretical Analysis

Speckle Photography Technique

In this technique, the source image considered as the input image is placed in front of the diffuser which is illuminated by coherent laser beam. In this case the transmitted complex amplitude is written as follows:

$$A(x,y) = d(x,y).g(x,y) \quad (1)$$

Segmentation using certain cross section from the above transmittance is obtained using circular aperture P (x, y) of diameter D = 2R. In this case, the transmitted complex amplitude becomes:

$$B(x,y) = d(x,y).g(x,y).P(x,y) \quad (2)$$

In the focal plane, we operate the Fourier transform upon equation (2), then we get the Fourier spectrum of the equation (1) as follows:

$$\beta(u,v) = D(u,v) \otimes G(u,v) \otimes h(u,v) \quad (3)$$

Where $\beta(u,v) = F.T.\{B(x,y)\}$,

$D(u,v) = F.T.\{d(x,y)\}$

$G(u,v) = F.T.\{g(x,y)\}$

$h(u,v) = F.T.\{P(x,y)\} = \frac{2J_1(w)}{w}$, is the Point Spread Function (PSF) for the circular aperture. The symbol $\otimes$ stands for the convolution operation.

The modulated speckle image represented by equation (3) is the convolution product of the ordinary speckle originated by the diffuser and the Fourier spectrum of the object information smeared by the PSF corresponding to the circular aperture. It is known that the segmentation using shifted cross section does not affect the speckle image since the displacement is equivalent to a phase shift in the Fourier plane and it has no effect upon the detected intensity. Only, the speckle image is dependent upon the aperture and the object information for certain random diffuser. Discrimination between the colon cancer and colon polyp is shown from the obtained speckle images. In addition, discrimination between different zones of cancerous colon image are shown referring to the speckle images.

Cascaded Interferometric Technique

The intensity of the two- beam interference obtained in the detector plane can be expressed as the modulus square as follows:

$$I = I_0\{1 + M\cos[\Phi(x,y;z) - \Psi(x,y)]\} \quad (4)$$

Where I(x, y; z) is the intensity of the modulated interference field at the point I(x , y) for object depth z, $I_0 = |R|^2 + |a|^2$, is the function that characterizes the mean intensity of the interference pattern and $M = (2a\ R)/[|R|^2 + |a|^2]$, is the function that determines the modulation of the interference signal. In this case, the obtained trigonometric function has straight line fringes modulated by the object phase information. The modulated intensity is rewritten in matrix form as follows:

$$I = I_0 \sum_{n=1}^{N} \sum_{m=1}^{M} \{1 + M \cos[\Phi(n\Delta x, m\Delta y; z) - \Psi(n\Delta x, m\Delta y)]\} \quad (5)$$

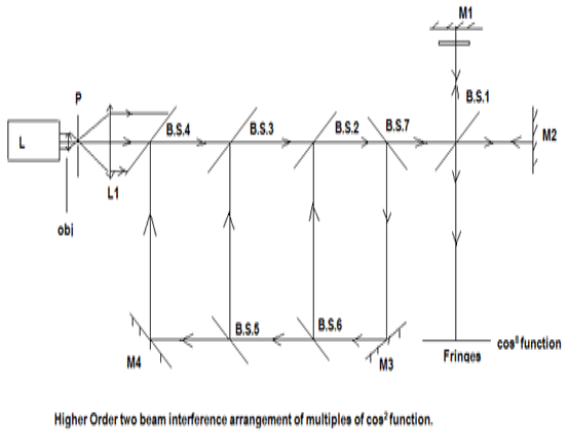

Figure3. *A cascaded higher order two beam interference where three loops are added to the original arrangement giving cos^8 function*

The coherent multiplication of two beam interference is governed by the feedback of the coherent laser beam that incident on the Michelson arrangement as shown in the figure (3). Hence, for the number of feedback passes (N) on the interferometer gives intensity distribution in the form [14]:

$$I_{feed\ back}(x, y; N) = I_0 cos^{2(N+1)}(\delta) \quad (6)$$

The ordinary two beam interference has intensity distribution extracted from equation (1), where N = 0(no feedback) as follows:

$$I_{ordinary}(x, y; 0) = I_0 cos^2(\delta) \quad (7)$$

For a single feedback N= 1

$$I_{feed\ back}(x, y; N = 1) = I_0 cos^4(\delta) \quad (8)$$

For two feedback light passes, N= 2

$$I_{feed\ back}(x, y; N = 2) = I_0 cos^6(\delta) \quad (9)$$

It is known that each feedback pass adds $\cos^2\delta$ to the original $\cos^2\delta$.

The fringe sharpness is conveniently measured by their full intensity width at half maximum (FWHM) [15]. In the case of ordinary two beam interference, the fringe sharpness is computed as:

$$\frac{I}{I_0} = \frac{1}{2} = cos^2(\delta_w) \quad (10)$$

In this case, the FWHM represented by (δ_w) is computed as follows:

$$\delta_w = cos^{-1}\left(\frac{1}{\sqrt{2}}\right) \quad (11)$$

While in case of multiple feedback of number of passes N, the FWHM is computed as follows:

$$\delta_w = cos^{-1}\left(\frac{1}{2(N+1)\sqrt{2}}\right) \quad (12)$$

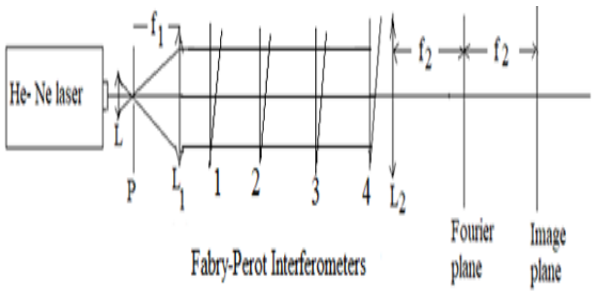

Figure4. *Multiple beam interferometers composed of four cascaded interferometers. L objective lens, P pinhole, and L1 converging lens where the elements L, P, and L1 render the laser beam spatially filtered and collimated. L2 is the Fourier transform lens of focal length f2, The Fourier and imaging planes are shown in the figure.*

In case of cascaded multiple beam interference as shown in the figure (4), the intensity distribution is the Airy distribution raised to the power of N, where N is the number of cascaded interferometers. Then, the intensity distribution is represented as follows [16, 17]:

$$I(\delta; R, N) = \left[\frac{T^4}{1 + R^4 - 2R^2\cos(\delta)}\right]^N \quad (13)$$

The maximum intensity is computed as:

$$I(\delta = 2\pi; R, N) = I_{max}(R, N) = \left[\frac{T^4}{(1-R^2)^2}\right]^N \quad (14)$$

Making use of equations (13, 14), the normalized intensity due to the cascaded multiple beam interference can be written as follows:

$$I_{normalized}(\delta; R, N) = \frac{I}{I_{max}} = \frac{1}{[1 + F\ sin^2(\frac{\delta}{2})]^N} \quad (15)$$

Where $F = \frac{4R^2}{(1-R^2)^2}$, is the coefficient of finesse. (16)

F is a measure of fringe sharpness and contrast.

Computation of Refractive Index from the Interference Image

Once the phase is determined across the interference field, the corresponding height distribution h (x, y) on the surface of corona virus can be determined [15] as follows:

$$h(x,y;z) = \frac{\lambda}{4\pi}\Phi(n\Delta x, m\Delta y; z) \qquad (17)$$

We have assumed the surface measured at normal incidence. Almost all interferometers used to measure surface height variations use phase-shifting techniques.

The optical path difference represents the height variation of the image, namely h (x, y, z) then the refractive index becomes [15]:

$$\mu(x,y) = 1 + \frac{d}{dz}[h(x,y,z)] \qquad (18)$$

The differentiation of the height distribution h (x, y, z) with respect to z give the differential fringe shift and the amplitude of the planar image a (x, y). Consequently, we finally get equation (19).

$$\mu(x,y)_{const.x} = 1 + a(x,y)\frac{\delta z}{\Delta z} \qquad (19)$$

The fringe shift is δz while the inter-fringe spacing isΔz at constant x, the fringes are assumed located in the x- y plane and z is the axis normal to the fringe system which represents the height depth and a (x, y) represents the amplitude of the image. In equation (18), h (x, y, z) = a (x, y). δz.

Results and Discussion

The speckle photography technique is applied on the source image of the colon cancer cells shown in the figure (5). A segment from the image taken from the figure (1) where the colon cancer and polyp are shown as in the figure (6). Speckle images corresponding to these images showed coarse speckle pattern for the cancerous colon as compared with the polyp finer speckle image as in the figure (7).

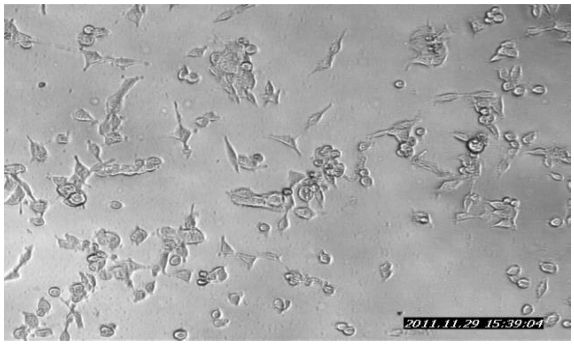

Figure5. *The source image of the colon cancer cells [12]*

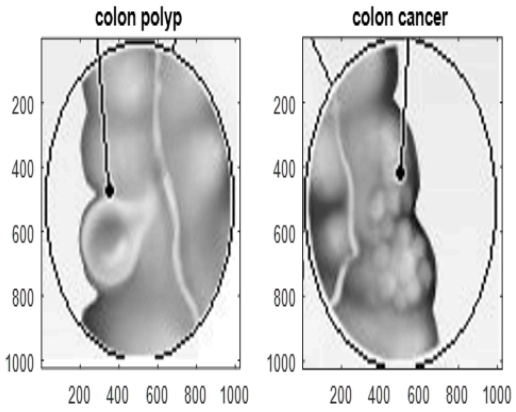

Figure6. *Colon polyp and colon cancer grayscale images of dimensions 1024× 1024 pixels.*

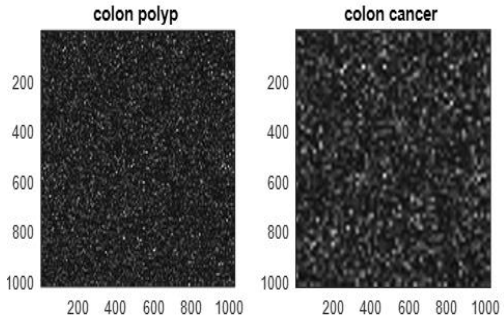

Figure7. *Speckle images corresponding to the colon polyp and colon cancer images of dimensions 1024× 1024 pixels.*

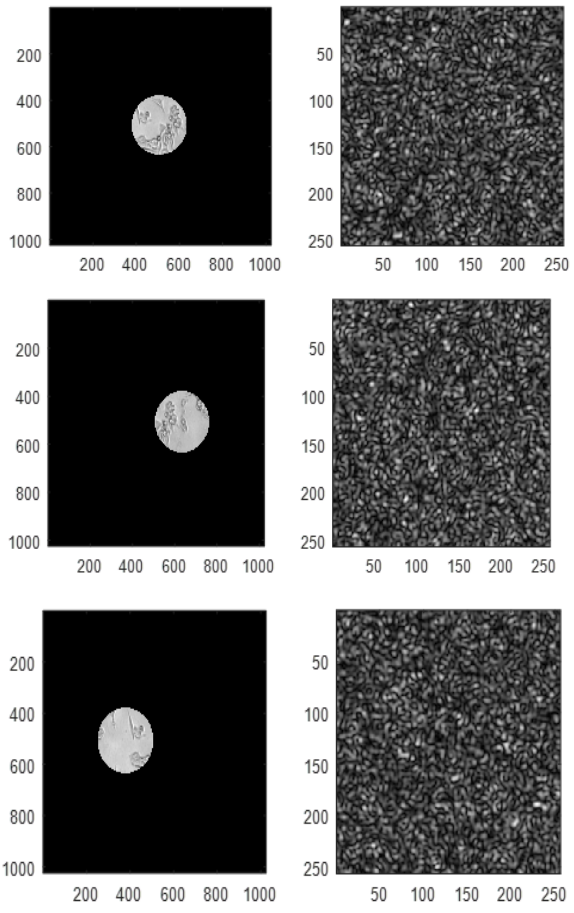

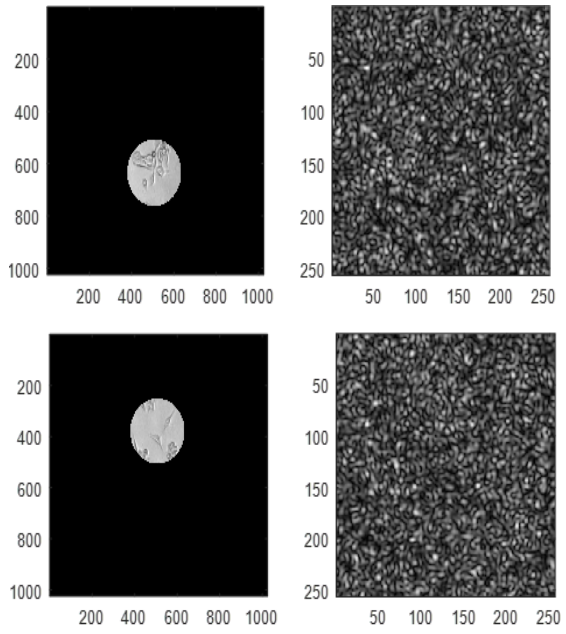

Figure8. *A set of five speckle images corresponding to segmented five different sections each of radius = 128 pixels where the 1st is centered at (512, 512) while the other four images are displaced by an amount d = 128 pixels. The diffuser has the same dimensions like the circular object.*

The speckle images are formed from the interference pattern of different scatters when a coherent laser beam is incident upon the diffuser. Modulated image is formed when an object information of transparency is placed directly before or after the diffuser. In this study, the speckle images corresponding to segmentation originated at different cross sections are constructed. A set of five speckle images corresponding to five different equal sections from the original image with radius = 128 pixels where the 1st is centered at (512, 512) while the other four images are displaced by an amount d = 128 pixels are shown in the figure (8). The diffuser has the same dimensions like the circular cross section taken from the object. The speckle images are dependent upon the information present in the cross section. Hence, we can discriminate easily between the different speckle images by the naked eye and quantitatively from its profiles.

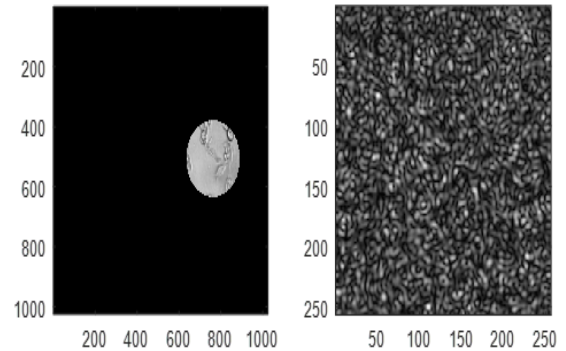

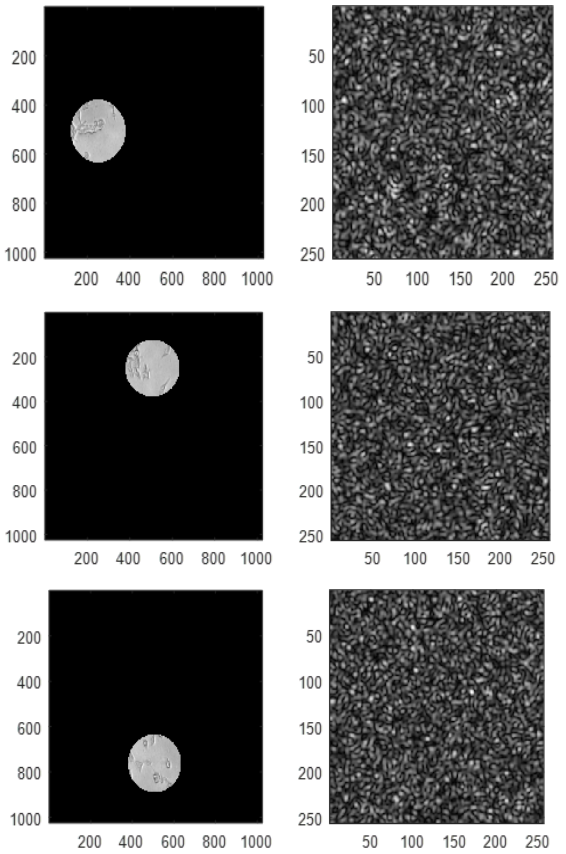

Figure9. *A set of four speckle images corresponding to segmented four different sections each of radius = 128 pixels, as shown in the figure (8), while the four images are displaced by an amount d = 256 pixels. The diffuser has the same dimensions like the circular object.*

Another set of four speckle images corresponding to four different equal sections each of radius = 128 pixels and displaced by an amount d = 256 pixels are shown in the figure (9). It is shown, referring to the speckle images that the different displacement which acquires different sections give different images. We will show quantitatively the differentiation referring to the corresponding profile shapes as shown in the figures (10, 11).

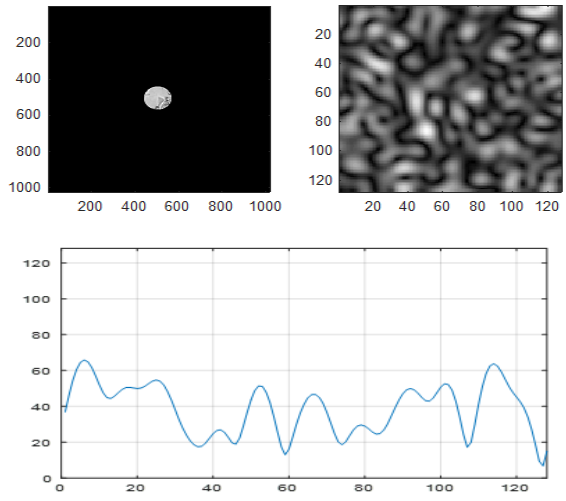

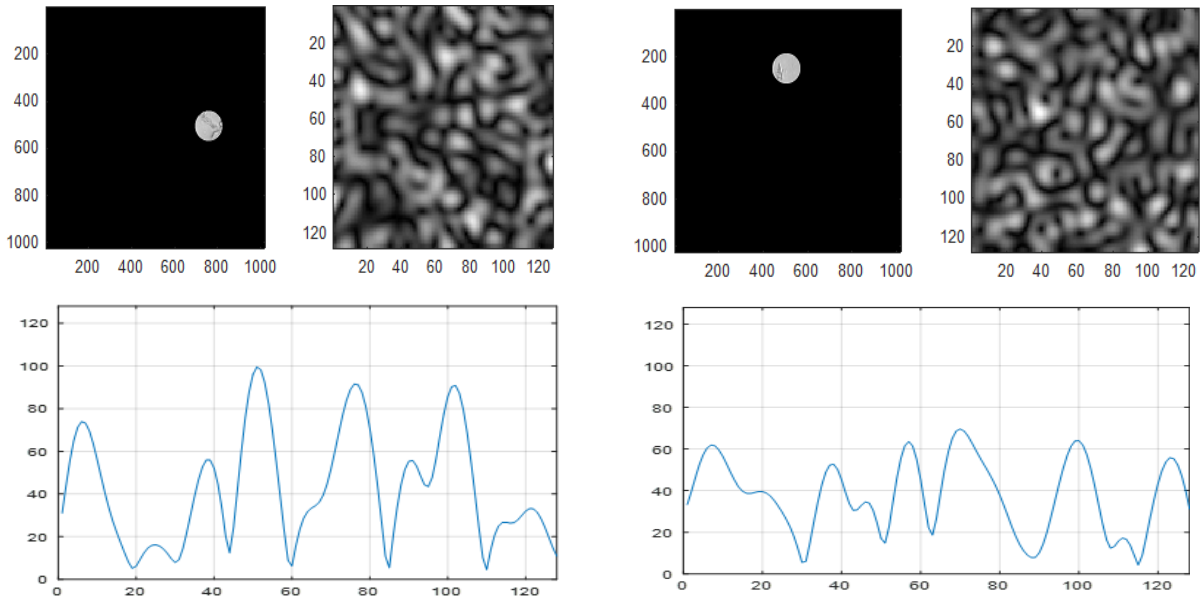

Figure10. *A set of five speckle images corresponding to five different equal sections each of radius = 64 pixels placed at (512, 512), (768, 512), (256, 512), (512, 768), and (512, 256) respectively. The diffuser has the same dimensions like the circular object. The profiles corresponding to each speckle image is shown below each figure.*

In figure (10), smaller cross section of radius = 64 pixels assumed in the formation of speckle images at different cross sections. A set of five speckle images corresponding to five different equal sections with radius = 64 pixels placed at (512, 512), (768, 512), (256, 512), (512, 768), and (512, 256) respectively are shown in the figure (10). The diffuser has the same dimensions like the circular object. The profiles corresponding to each speckle image are plotted below each figure. It is shown that the speckle image profiles are completely different since each speckle image is formed from the convolution product of the ordinary speckle and the Fourier spectrum corresponding to the outlined cross section from the object.

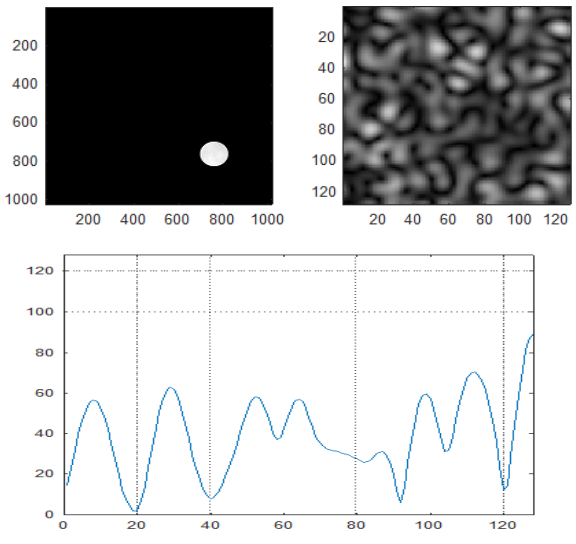

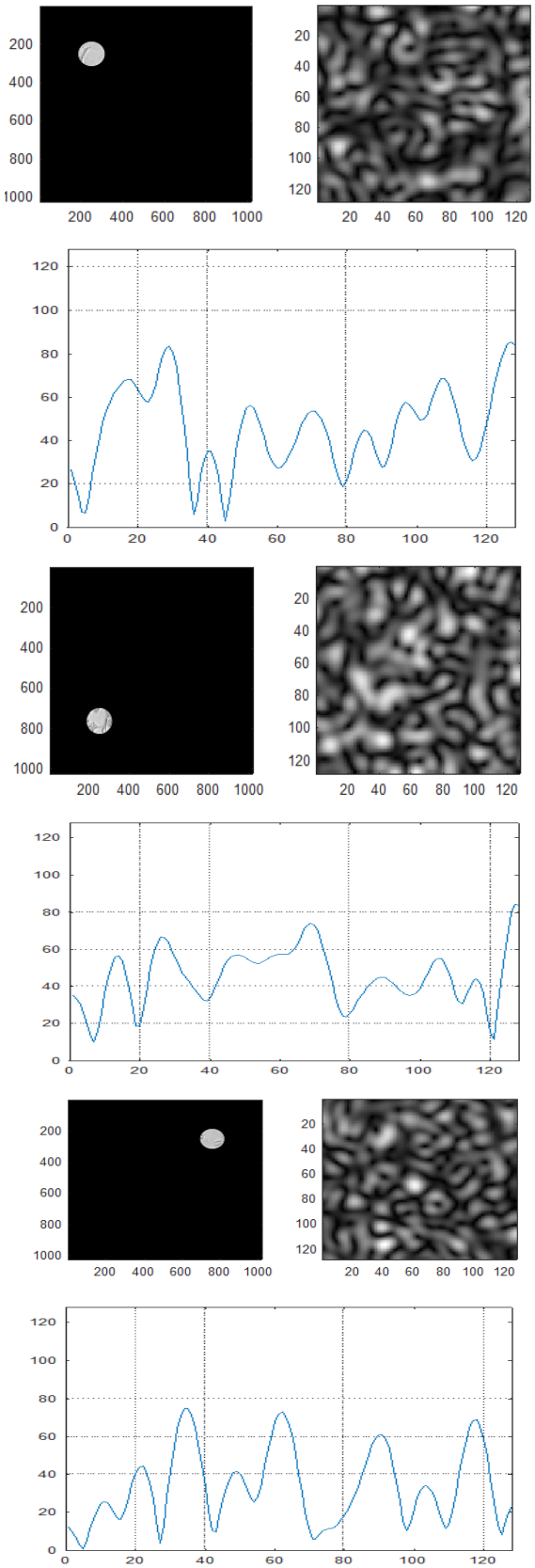

Figure11. *In the left, four images of the colon circular cross section of radius = 64 pixels displaced along the diagonal and located at (768, 768), (256, 256), (256, 768), and (768, 256) respectively. In the right, the corresponding speckle images are shown. The profiles corresponding the speckle images at 64 pixels are shown below the corresponding speckle image.*

Another set of speckle image originated from cross section placed along the diagonals are plotted as in the figure (11). In the left, four images of the colon circular cross section of radius = 64 pixels displaced along the diagonal and located at (768, 768), (256, 256), (256, 768), and (768, 256) respectively. In the right, the corresponding speckle images are shown. The profiles corresponding the speckle images at 64 pixels are plotted below the corresponding speckle image. Referring to the speckle profile plots corresponding to each cross section, we can discriminate between the cross sections from the speckle image information.

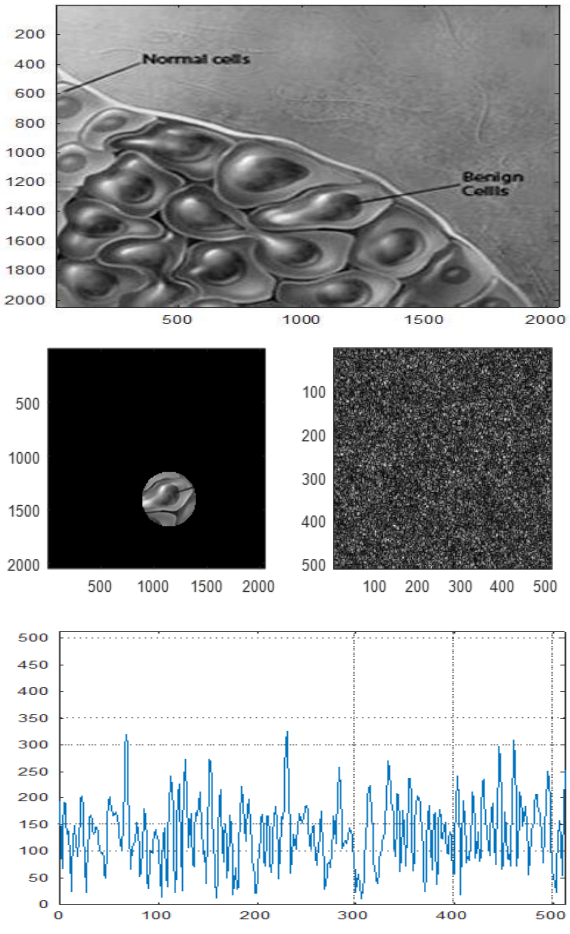

Figure12. *In the upper, benign and normal cells are seen in the image of colon. In the middle, cross section focused on the benign cell and the corresponding speckle image are in the same plot. In the lower, the profile corresponding to the speckle image taken at 256 pixels is shown.*

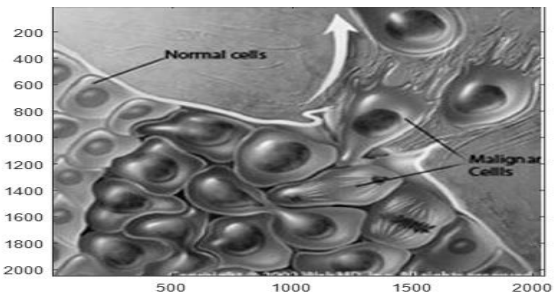

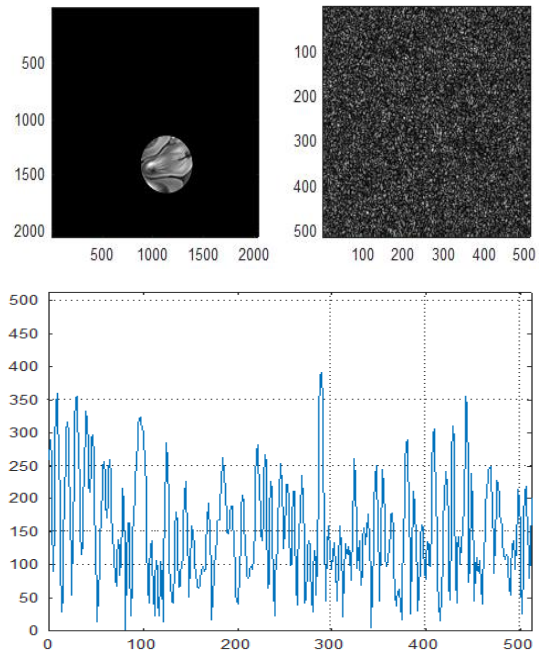

Figure13. *In the upper, malignant and normal cells are seen in the image of colon. In the middle, cross section focused on the malignant cell and the corresponding speckle image are in the same plot. In the lower, the profile corresponding to the speckle image taken at 256 pixels is shown.*

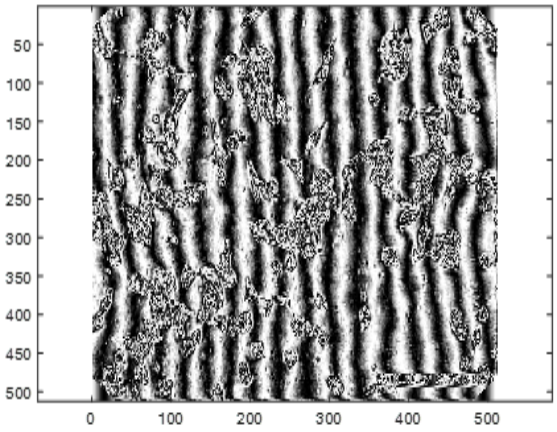

Figure14- a. *Modulated cancerous cells using ordinary two beam interference. The contour corresponding to the cancerous cells in the colon is shown.*

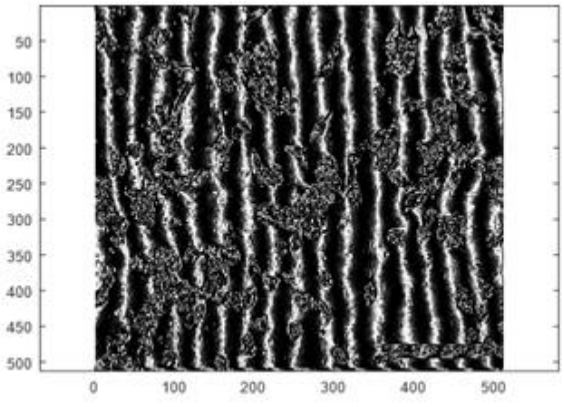

Figure14- b. *Modulated cancerous cells using ordinary multiple beam interference*

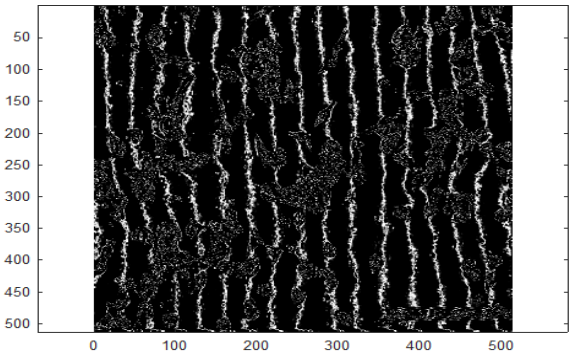

Figure14- c. *Modulated cancerous cells using cascaded multiple beam interference of N = 5.*

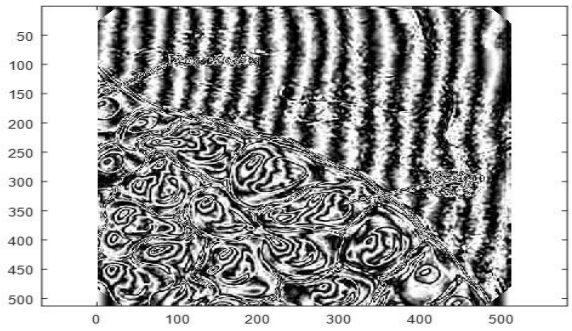

Figure15- a. *Benign and normal cells in the human colon modulated with two beam interference corresponding to the source image shown in the figure (12).*

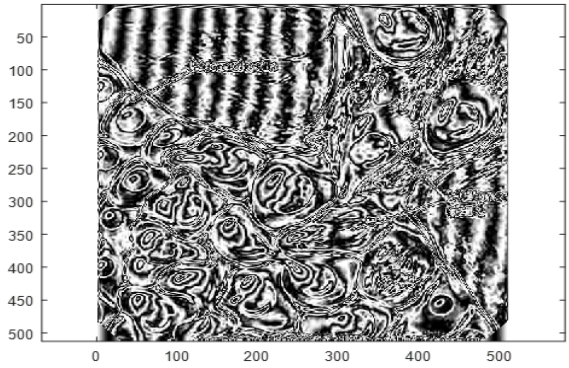

Figure15-b. *Malignant and normal cells in the human colon modulated with two beam interference corresponding to the source image shown in the figure (13).*

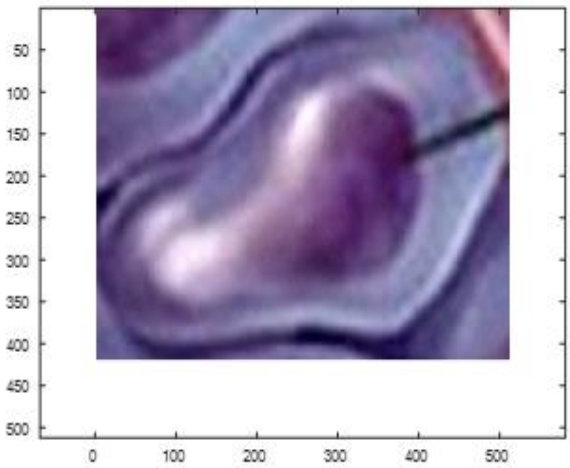

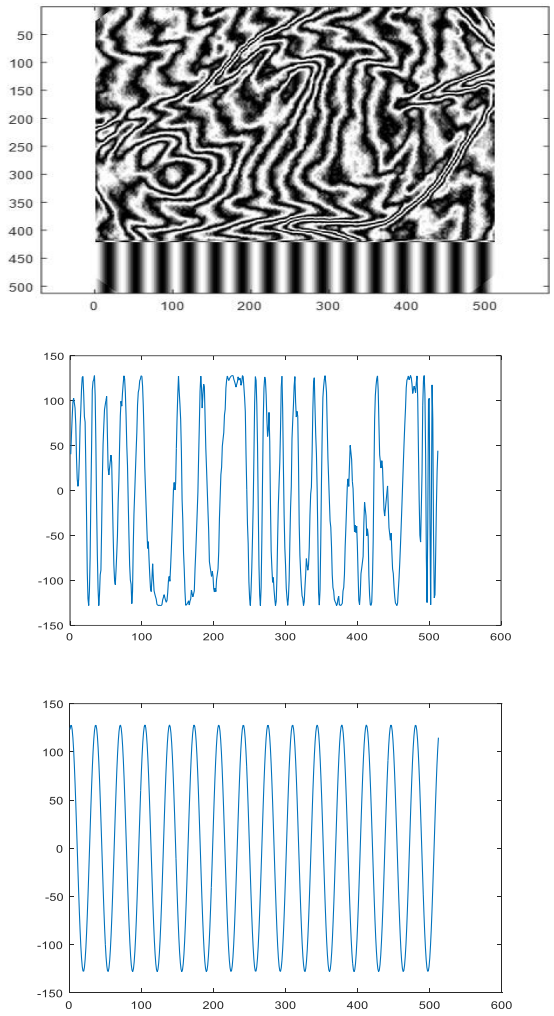

Figure16- a. *In the 1st row, a benign cell of colon is shown, in the 2nd row the corresponding modulated fringe pattern, while in the 3rd row the profile plot of the benign fringe pattern at 256 pixels and in the 4th row plot of ordinary two beam interference is given.*

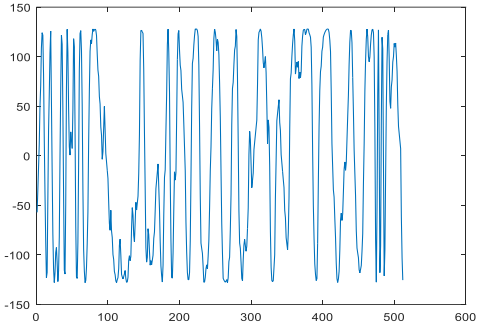

Figure16- b. *In the above, a malignant cell of colon is shown, in the middle the corresponding modulated fringe pattern, while in the lower the profile plot corresponding to the malignant fringe pattern at 256 pixels.*

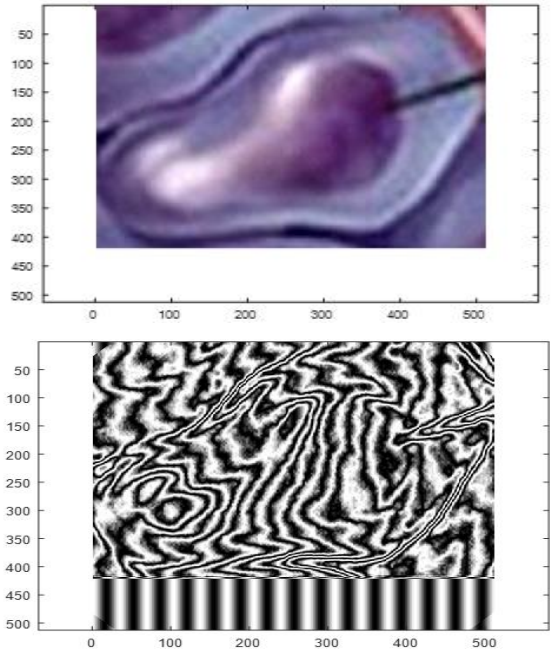

Figure17- a. *Benign colon cell modulated by ordinary multiple beam interference*

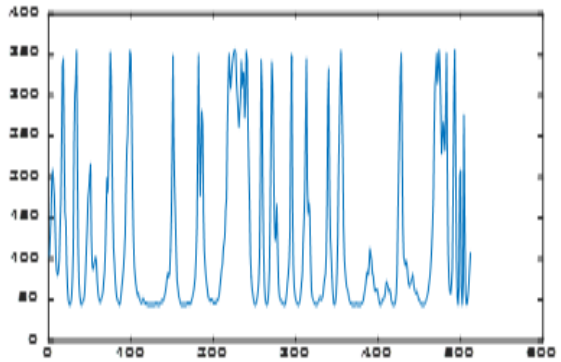

Figure17- b. *Profile corresponding to the benign cell modulated by ordinary multiple beam interference of N= 1 at horizontal section at 256 pixels.*

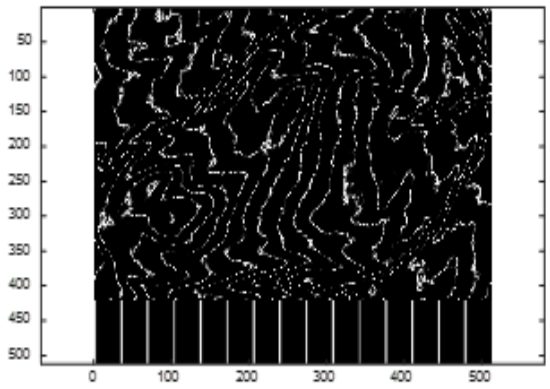

Figure17- c. *Benign colon cell modulated by cascaded multiple beam interference of N= 10.*

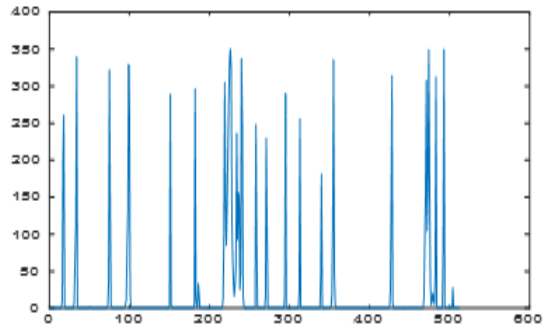

Figure17- d. *Profile corresponding to the benign cell modulated by cascaded multiple beam interference of N = 10 at horizontal section at 256 pixels.*

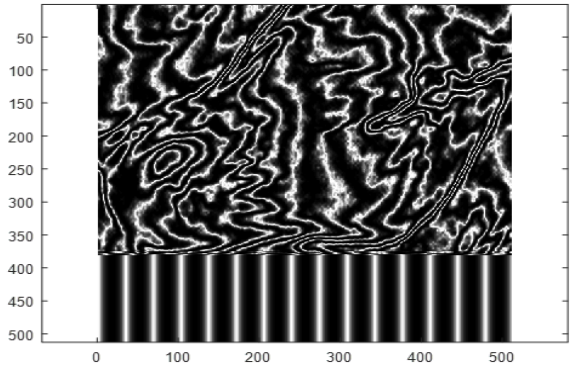

Figure18-a. Malignant *colon cell modulated by ordinary multiple beam interference*

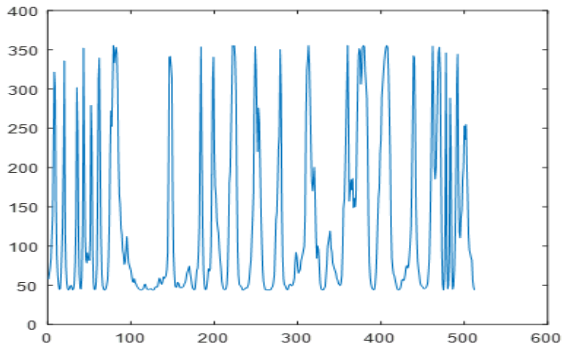

Figure18- b. *Profile corresponding to the benign cell modulated by ordinary multiple beam interference of N= 1 at horizontal section at 256 pixels.*

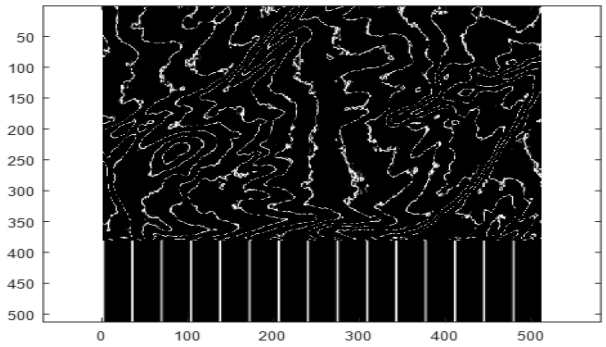

Figure18- c. *Malignant colon cell modulated by cascaded multiple beam interference of N= 10.*

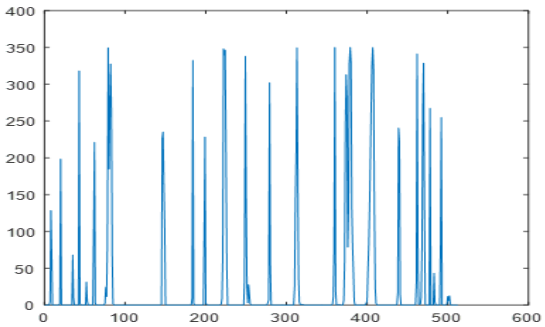

Figure18- d. *Profile corresponding to the malignant cell modulated by cascaded multiple beam interference of N = 10 at horizontal section at 256 pixels.*

Discrimination between benign and malignant cells is verified by focusing on the interested cross sections including the benign cell in the colon as shown in the figure (12). Then, we get the corresponding speckle image and plot the profile shape at the certain zone at 256 pixels. We repeat the job for the malignant cell in the colon as shown in the figure (13). The profile shape corresponding to the formed speckle image is taken at the same zone at 256 pixels. Comparing the two profiles we find a great difference is found which is attributed to the cell shape since the random diffuser used in the formation of the speckle is the same in the two figures (12, 13). The contour of the colon

cancerous cells is detected using two beam interference as shown in the figure (14- a). It is improved by using cascaded multiple beam interference and compared with ordinary interference pattern as shown in the figure (14 b, c).Benign and normal cells in the human colon modulated with two beam interference corresponding to the source image as in the figure (12) is shown in the figure (15- a). While the malignant cells modulated with the same ordinary two beam interference is shown in the figure (15- b). In the 1st row, in figure (16- a), a benign cell of colon is shown, in the 2nd row the corresponding modulated fringe pattern originated from ordinary two beam interference, while in the 3rd row the profile plot of the benign fringe pattern at 256 pixels and in the 4th row plot of ordinary two beam interference is given. In the above, as shown in the figure (16- b), a malignant cell of colon is shown, in the middle the corresponding modulated fringe pattern, while in the lower the profile plot corresponding to the malignant fringe pattern at 256 pixels. The improved sharp fringe pattern attained as shown in the figures (17- a, 16- a) using multiple beam interference corresponding to the benign and malignant cells is further improved using cascaded interference as shown in the figures (15- c, 18- c). The corresponding plots are given as shown in the figures (17- b, 18- b) for the ordinary pattern and as shown in the figures (17- d, 18- d) for the cascaded interference pattern.

The fringe shift corresponding to the benign and malignant cells is computed accurately from the sharp profiles obtained in case of cascaded multiple beam interference as shown in the figures (17- d) for the benign cell and as shown in the figure (18- d) for the malignant cell. The fringe sharpness is proportional to the number of cascaded passes N.

The height or the surface topography corresponding to the benign and malignant colon cells is extracted from the fringe shift for certain amplitude a (x, y) in the image as shown in the tables (1, 2). In addition, the corresponding refractive index is computed using approximate equation (19).

Table1. *Benign cells interference results at horizontal line at 200 pixels, the inter-fringe spacing ΔZ = 34 pixels compared with fringe shift shown in the plots.*

Z	Z_{image}	$\delta Z = Z - Z_{image}$	$\mu = 1 + \delta Z/\Delta Z$
34	18	16	1.4700
68	34	34	2.0000
102	75	28	1.8235
136	102	34	2.0000
170	151	19	1.5588
204	182	22	1.6470
238	234	4	1.1176
272	258	14	1.4117
306	272	34	2.0000

Table2. *Benign cells interference results at horizontal line at 200 pixels, the inter-fringe spacing ΔZ = 34 pixels compared with fringe shift shown in the plots.*

Z	Z_{image}	$\delta Z = Z - Z_{image}$	$\mu = 1 + \delta Z/\Delta Z$
34	20	14	1.4117
68	48	20	1.5882
102	82	20	1.5882
136	117	19	1.5588
170	147	23	1.6765
204	198	6	1.1765
238	222	16	1.4700
272	249	23	1.6765
306	279	27	1.7941

CONCLUSION

Firstly, the speckle imaging of the benign and malignant cancerous cell of colon is proved a powerful technique in discrimination since the obtained profiles are completely different. We used the same random diffuser of equal dimensions like the source image.

Secondly, we used ordinary two beam and multiple- beam in the discrimination between the benign and malignant colon cells. The fringe shift showed a difference in both cases. Further improvement in the sharpness of the fringe shift is attained by using cascaded models of two and multiple beam interference. It was shown that the fringe sharpness is improved with number of cascaded passes N [14- 17]. This is useful in the investigation of the fringe shift which gives more accurate results.

REFERENCES

[1] Medical Net. Inc. 2010.

[2] Jawad N., Direkze N., and Leedham SJ., Recent Results in Cancer Research 185 (2011)99- 105, Inflammatory bowel disease and colon cancer.

[3] Macaskill, B.A., Chan, P., Katelaris, S.F., Irwig, P.H., Most, L.: bowel cancer symptoms do not indicate colorectal cancer and polyps: a systematic review. BMC Gastroenterology 11(65) (2011), doi:10.1186/1471-230X-11-65

[4] Astin, M., Griffin, T., Neal, R.D., Rose, P., Hamilton, W.: The diagnostic value of symptoms for colorectal cancer in primary care: a systematic review. The British Journal of General Practice: The Journal of the Royal College of General Practitioners 61(586), 231–243 (2011), doi:10.3399/bjgp11X572427

[5] Cunningham, D., Atkin, W., Lenz, H.J., Lynch, H.T., Minsky, B., Nordlinger, B., Starling, N.: Colorectal cancer. Lancet 375 (9719), 1030–1047 (2010), doi:10.1016/S0140 -6736(10)60353-4

[6] Diggsa, D.L., Myersa, J.N., Banksa, L.D., Niaza, M.S., Hoodb, D.B., Roberts, L.J., Ramesha, A.: Influence of dietary fat type on benzo (a)pyrene [B(a)P] biotransformation in a B(a) P-induced mouse model of colon cancer. The Journal of Nutritional Biochemistry 24(12), 2051–2063 (2013)

[7] Eadie, L.H., Reid, C.B., Fitzgerald, A.J., Wallace, V.P.: Optimizing multi-dimensional terahertz imaging analysis for colon cancer diagnosis. Expert Systems with Applications 40(6), 2043 –2050 (2013)

[8] Bochenek, A., Reicher, M.: Anatomia Człowieka. 2, Wydawnictwo Lekarskie PZWL, pp. 239–267 (2004).

[9] Anna Wójcicka1, et. al, Advances in intelligent systems and computing, vol. 283 (2014). ISBN: 978-3-319-06592-2.

[10] A.M. Hamed, Int. J. Innovative Res. in Eng. and Management (IJIREM) .3 (2016) 125- 133, Discrimination between normal and diseased stomach using speckle imaging.

[11] A.M. Hamed, Int. J. Innovative Res. in Computer Science and Tech (IJIRCST), 4 (2016)38- 45, Investigation of SIDA Virus (HIV) images using interferometry and speckle techniques.

[12] A.M. Hamed, Opt. and Photonics J. 6 (2016)75- 86, Image processing of corona virus using interferometry.

[13] A.M. Hamed and T. A. Al-Saeed, IJPOT 2 (2016) 6- 12, Reconstruction of the corneal layers affected by a periodic noise Application on microscopic interferometry

[14] A.M. Hamed, IJPOT 3(2017), A modified Michelson interferometer and an application on microscopic imaging.

[15] A.M. Hamed, IJPOT 3 (2017), Processing of the retinal artery image using higher orders of two beam interference.

[16] A.M. Hamed, Int. J. Innovative Res. in Eng. and Management (IJIREM), 5 (2018) 189- 195, Sharp fringes using cascaded Multiple beam interferometers. Application on Kidney images.

[17] A.M. Hamed, Int. J. Innovative Res. in Eng. and Management (IJIREM), 5 (2018) 173- 181, Recognition of some modulated apertures using the Cascaded Fabry- Perot Interferometer (CFPI).

[18] A.M. Hamed, International Journal of Emerging Engineering Research and Technology (IJEERT) vol. 7, issue 1 (2019) 1-12, Image Processing of Mammographic Images using Holography and Interferometry.

[19] A.M. Hamed, International Journal of Advanced Research in Electronics and Communication Engineering (IJARECE) 8 (2019) 1- 8, Discrimination between microscopic images and its reconstruction using intelligent digital speckle images.

Citation: *A.M. Hamed, "Investigation of Colon Using Speckle and Cascaded Interferometric Techniques", International Journal of Emerging Engineering Research and Technology, 8(6), 2020, pp. 1-12.*